Applied Mathematical Modelling 37 (2013) 5080–5091

Contents lists available at SciVerse ScienceDirect

Applied Mathematical Modelling

journal homepage: www.elsevier.com/locate/apm

Dielectric waveguides of arbitrary cross sectional shape

Theodoros P. Horikis

Department of Mathematics, University of Ioannina, Ioannina 45110, Greece

ARTICLE INFO

Article history:
Received 13 February 2012
Received in revised form 17 September 2012
Accepted 15 October 2012
Available online 26 October 2012

Keywords:
Finite differences
Immersed interface method
Arbitrary cross sections
Full vectorial interface conditions
Bragg fibers

ABSTRACT

Numerical guided mode solutions of arbitrary cross sectional shaped waveguides are obtained using a finite difference (FD) technique. The standard FD scheme is appropriately modified to capture all discontinuities, due to the change of the refractive index, across the waveguides' interfaces taking into account the shape of each interface at the same time. The method is applied to the vector Helmholtz equation formulated to describe the electric or magnetic fields in the waveguide (one field is retrieved from the other through Maxwell's equations). Computational cost is kept to a minimum by exploiting sparse matrix algebra. The waveguides under study have arbitrary cross sectional shape and arbitrary refractive index profile.

1. Introduction

With the continuously increasing interest in fiber optic and integrated optic communication techniques has come the need to know in great detail the properties of dielectric waveguides. Optical waveguide theory is still under development and our knowledge of how cross sectional shape influences propagation is still rather small. Indeed, analytical solutions of Maxwell's equations exist only for the planar waveguide and for fibers of circular cross section. The difficulty is not confined to solving Maxwell's equations. Even the comparatively simple scalar wave equation has analytical (closed form) solutions only for cross sections that are nearly circular or for graded refractive-index profiles that are essentially unphysical.

The case of circular fibers has almost been exhausted in the literature. Light confinement due to cylindrical Bragg reflection instead of total internal reflection was first proposed more than three decades ago [1] and gave birth to the so-called Bragg fibers. These fibers attract considerable interest because of their ability to guide light in an air core. The key to making these fibers confine light efficiently, i.e., have low absorption loss and a high threshold power for nonlinear effects, is to use materials with a high index contrast [2–5]. However, the high index contrast and the layered structure that gives these fibers their unique properties also makes them difficult to model. Due to their circular symmetry these fibers can be modeled in polar coordinates by 1D equations. As a result, several methods have been proposed to study their properties, including asymptotic analysis [6], the transfer matrix method [7], matrix formulas involving Bessel functions [8], and Galerkin numerical methods [9]. A comparative analysis of the most commonly used methods has also been published [7], demonstrating the efficiency and the limitations of each method.

Particular interest has also been shown in the study of elliptic core fibers [10,11]. Fibers of elliptical cross section exhibit a rich variety of modal characteristics and have been studied both numerically [10–14] and analytically [15,16]. Indeed, single-mode elliptic core fibers which can maintain the polarization state of the propagating beam over long distances have a large number of applications. However, in these fibers the propagation characteristics can only be determined numerically since closed form solutions are represented by Mathieu functions which are difficult to handle [15].

E-mail address: horikis@uoi.gr

0307-904X/$ - see front matter © 2012 Elsevier Inc. All rights reserved.
http://dx.doi.org/10.1016/j.apm.2012.10.025

Despite the great effort spent in developing techniques to model circular waveguides our knowledge of the effects of the arbitrary cross sections of a waveguide is small. Indeed, none of the above methods can be directly applied to these problems. Attempts to overcome this difficulty have been proposed in the literature ranging from integral representations of the field components [17] and Galerkin [18] to asymptotic [19] and finite element [20] methods. The purpose of this article is to address the analysis of such problems in a simple and efficient manner.

Mathematically these problems are formulated as Helmholtz type equations on a domain defined by the shape of the fiber's cross section; the cross section defines the shape of the boundary where the boundary conditions are applied. This is a challenging problem on its own, but due to the change of the refractive index across the interfaces the coefficients of the equations are also discontinuous or even singular making the problem impossible to study analytically. In fact, these problems are often called interface problems since their input data (such as the coefficients of differential equations, source terms etc.) are discontinuous or even singular across one or several interfaces. The solution to an interface problem is typically non-smooth or even discontinuous across the interfaces. Interface problems occur in many physical applications, particularly for free boundary/moving interface problems, such as, the modeling of the Stefan problem of solidification process and crystal growth, composite materials, multi-phase flows, cell and bubble deformation, and many others [21].

Recently, a second-order finite difference (FD) approach based upon the immersed interface method [22] (IIM) was introduced to analyze the modes of these fibers [23,24]. This approach has two additional advantages over standard Galerkin methods [9]. First of all, the scheme does not need to be modified significantly if different boundary conditions are used, thus allowing to calculate all higher modes of a fiber without any modifications. Methods based upon the Galerkin method typically require using a set of basis functions that naturally satisfy the boundary conditions, hence the solution must be reformulated in a significant way if they change. More importantly, the IIM depends only upon the index values and not on any specific functional representation of solutions; cumbersome integrations or finding roots of nontrivial functions, such as Bessel functions (even when asymptotically approximated), are avoided.

It should also be noted that the FD approach has also been considered for this problem in different contexts. In Ref. [25] a high order matched interface and boundary method is used while in [26] a combined matching boundary condition and Taylor series expansion is implemented. In both cases, a local change in polar coordinates is needed and as such the matching conditions across interfaces have to be appropriately defined. While both approaches are of higher order accuracy they may pose a limitation when dealing with multiple interfaces. Indeed, the first is based on the use of fictitious nodes as an important step in enforcing the jump/boundary conditions while the latter needs 15 sampled points to establish 15 equations for each polarization in fourth order and 28 points to solve derivatives up to sixth order. As such, and depending on the width of each layer in the waveguide one may need additional grid points (a finer grid) thus increasing computational time.

Techniques based on finite differences carry an additional advantage. Using sparse matrix algebra one can significantly lower computational time. The goal is to identify the grid points the interface falls in between and appropriately correct the standard FD coefficients in a way described below to take into account the effects of the interfaces. Remarkably, these corrections are found to be solutions of linear algebraic systems of equations. Thus, the matrix remains sparse (since no additional elements are added, only existing ones are corrected) and computational time is kept to a minimum.

The original formulation [22] of the IIM does not consider eigenvalue problems such as the problems of interest here. Hence, in order to deal with waveguide problems for Bragg fibers, the method must be extended to handle eigenvalue problems described by linear differential operators. Moreover, a further extension is also necessary to include coupled equations like the ones describing the two polarization components of the electromagnetic field.

2. Formulation

For monochromatic fields with angular frequency ω and time dependence $\exp(i\omega t)$, Maxwell's equations can be written in cartesian coordinates as [18]

$$\nabla \times \mathbf{H} = i\omega n^2 \varepsilon_0 \mathbf{E}, \tag{1a}$$

$$\nabla \times \mathbf{E} = -i\omega \mu_0 \mathbf{H}, \tag{1b}$$

where $\mathbf{E}$ and $\mathbf{H}$ are the electric and magnetic field vectors, ε_0 and μ_0 are the electric permittivity and the magnetic permeability of vacuum and $n = n(x,y)$ the refractive index. Taking the curl of Eq. (1a) and substituting for $\nabla \times \mathbf{E}$ from the second equation we have

$$\nabla \times (\nabla \times \mathbf{H}) = n^2 k^2 \mathbf{E},$$

with $k = \omega\sqrt{\varepsilon_0 \mu_0}$. Using the identity

$$\nabla \times (\nabla \times \mathbf{H}) = \nabla(\nabla \cdot \mathbf{H}) - \nabla^2 \mathbf{H}$$

and $\nabla \cdot \mathbf{H} = 0$ we obtain the following vector equation for the magnetic field

$$\nabla^2 \mathbf{H} + k^2 n^2 \mathbf{H} + \left[\frac{\nabla n^2}{n^2} \times (\nabla \times \mathbf{H})\right] = \mathbf{0}$$

Since we are only interested in the guided mode solutions whose z dependence can be written as $\exp(-i\beta z)$, the Laplace operator assumes the form $\nabla^2 = \partial^2/\partial x^2 + \partial^2/\partial y^2 - \beta^2$. Due to the fact that $n = n(x,y)$ and hence $\partial n/\partial z = 0$ the transverse components of $\mathbf{H}$, i.e. H_x and H_y satisfy the coupled equations

$$\frac{\partial^2 H_x}{\partial x^2} + \frac{\partial^2 H_x}{\partial y^2} - 2\frac{\partial \ln n}{\partial y}\left(\frac{\partial H_y}{\partial x} - \frac{\partial H_x}{\partial y}\right) + k^2 n^2 H_x = \beta^2 H_x, \tag{2a}$$

$$\frac{\partial^2 H_y}{\partial x^2} + \frac{\partial^2 H_y}{\partial y^2} - 2\frac{\partial \ln n}{\partial x}\left(\frac{\partial H_y}{\partial x} - \frac{\partial H_x}{\partial y}\right) + k^2 n^2 H_y = \beta^2 H_y. \tag{2b}$$

We choose to work with the magnetic field, $\mathbf{H} = (H_x, H_y)^{\mathbf{T}}$, because it is continuous on the interfaces. The electric field is not, but can be obtained from the following equations

$$E_x = \frac{1}{\omega\varepsilon_0\beta}\left\{k^2 H_y - \frac{\partial}{\partial x}\left[\frac{1}{n^2}\left(\frac{\partial H_x}{\partial y} - \frac{\partial H_y}{\partial x}\right)\right]\right\}, \tag{3a}$$

$$E_y = -\frac{1}{\omega\varepsilon_0\beta}\left\{k^2 H_x + \frac{\partial}{\partial y}\left[\frac{1}{n^2}\left(\frac{\partial H_x}{\partial y} - \frac{\partial H_y}{\partial x}\right)\right]\right\}, \tag{3b}$$

$$E_z = \frac{i}{n^2\omega\varepsilon_0}\left(\frac{\partial H_x}{\partial y} - \frac{\partial H_y}{\partial x}\right), \tag{3c}$$

$$H_z = \frac{i}{\omega\mu_0}\left(\frac{\partial E_y}{\partial x} - \frac{\partial E_x}{\partial y}\right), \tag{3d}$$

As usual all fields are evanescent outside the waveguide, i.e. $\mathbf{H}(r) = 0$ as $r(=\sqrt{x^2+y^2}) \to \infty$. For a more detailed derivation and the physical properties of these fields and related equations we refer the reader to Refs. [18,27].

3. Numerical scheme

We begin with Maxwell's equations for the x and y components of the magnetic field, H_x and H_y, as formulated in the previous section by Eq. (2b). We focus on these two field components, since the components of the electrical field, E_x, E_y and E_z, as well as the longitudinal magnetic field, H_z, can be recovered from H_x and H_y using Eq. (3d). Neglecting terms that involve derivatives of the refractive index, Eq. (2b) are written is vector form as

$$\mathbf{H}_{xx} + \mathbf{H}_{yy} + k^2 n^2 \mathbf{H} = \beta^2 \mathbf{H}$$

where $\mathbf{H} = (H_x, H_y)^{\mathbf{T}}$ and the subscripts under vectors denote differentiation. The effects of these terms will be added to the continuity conditions the fields must satisfy across interfaces. The domain of integration is a square, say $[a,b]\times[a,b]$ and a uniform grid

$$x_i = a + \frac{b-a}{n} i, \quad y_j = a + \frac{b-a}{n} j, \quad i,j = 1,2,\ldots,n$$

is considered. The finite (central) difference approximation of Eq. (2b) is written as

$$\Gamma_1 \mathbf{H}_{i-1,j} + \Gamma_2 \mathbf{H}_{i,j-1} + \Gamma_3 \mathbf{H}_{i,j} + \Gamma_4 \mathbf{H}_{i+1,j} + \Gamma_5 \mathbf{H}_{i,j+1} = \beta^2 \mathbf{H}_{i,j},$$

with

$$\Gamma_1 = \Gamma_2 = \Gamma_4 = \Gamma_5 = \frac{1}{h^2} I_2, \quad \Gamma_3 = \left(-\frac{4}{h^2} + k^2 n_{i,j}^2\right) I_2,$$

where I_2 is the 2×2 identity matrix and $h = (b-a)/n$.

This scheme is not applicable to all points since terms that are singular or discontinuous have been neglected. In order to take into account these terms we reformulate separating all points into "regular" and "irregular". We need to determine the Γ's at all irregular points; the FD coefficients are determined as above for all regular points. A regular point (i,j) is a point such that the interface does not come between any points in the standard five point stencil centered at (i,j); all other points are irregular. This is illustrated in Fig. 1.

When an interface lies within the five-point stencil, we expand all fields about some point (x_i^*, y_j^*) that belongs to the interface. In our approach this point is determined to be the closest point of the interface to the irregular point. The superscripts $(-)$ and $(+)$ will now denote the limiting values of a function from inside or outside the interface (cf. Fig. 1). For example, any field H at the point (x_i, y_j) (labeled "3" in the figure), is expanded as

$$H(x_i,y_j) = H^- + (x_i - x_i^*)H_x^- + (y_j - y_j^*)H_y^- + \frac{1}{2}(x_i - x_i^*)^2 H_{xx}^- + \frac{1}{2}(y_j - y_j^*)^2 H_{yy}^- + (x_i - x_i^*)(y_j - y_j^*)H_{xy}^-,$$

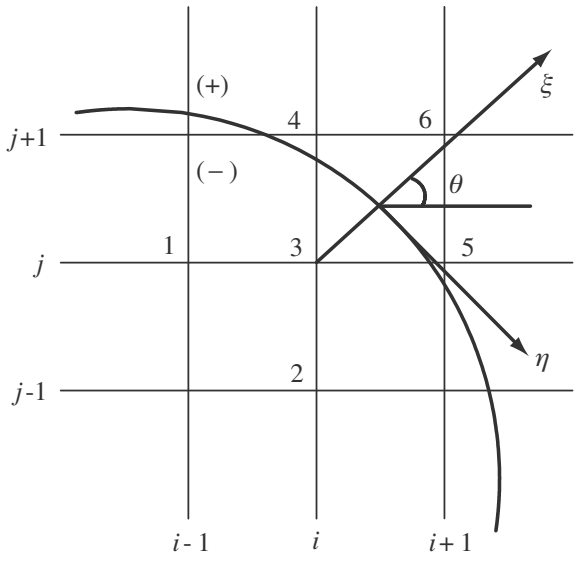

Fig. 1. The geometry of an irregular point (x_i, y_j), here labeled "3".

where we denote $H^- = H_{i,j} = H(x_i, y_j)$ and similarly for the derivatives of H^-. At the point (x_{i+1}, y_j) (labeled "5" in the figure), which lies on the $(+)$ side, fields are expanded in a similar manner as

$$H(x_{i+1}, y_j) = H^+ + (x_{i+1} - x_i^*)H_x^+ + (y_j - y_j^*)H_y^+ + \frac{1}{2}(x_{i+1} - x_i^*)^2 H_{xx}^+ + \frac{1}{2}(y_j - y_j^*)^2 H_{yy}^+ + (x_{i+1} - x_i^*)(y_j - y_j^*)H_{xy}^+,$$

where we denote $H^+ = H_{i+1,j} = H(x_{i+1}, y_j)$ and similarly for the derivatives of H^+. The expansion about (x_{i+1}, y_j) involves the values of the field and its derivative at the (+) side while the expansion around (x_i, y_j) the relative values at the $(-)$ side. To replace the one or the other, depending on the side of the interface we are, we use continuity or matching conditions across the interface. The continuity conditions on the interface demand that: the fields are continuous

$$\mathbf{H}_x^- = \mathbf{H}_x^+ \quad \textbf{and} \quad \mathbf{H}_y^- = \mathbf{H}_y^+,$$

the z-components of each field (here E_z) are continuous

$$\frac{1}{n_1^2}\left(\frac{\partial H_x^-}{\partial y} + \frac{\partial H_y^-}{\partial x}\right) = \frac{1}{n_2^2}\left(\frac{\partial H_x^+}{\partial y} + \frac{\partial H_y^+}{\partial x}\right)$$

and the tangential derivatives are continuous

$$\frac{\partial H_x^-}{\partial x} + \frac{\partial H_y^-}{\partial y} = \frac{\partial H_x^+}{\partial x} + \frac{\partial H_y^+}{\partial y},$$

where

$$n(x,y) = \begin{cases} n_1, & \text{inside the interface} \\ n_2, & \text{outside the interface} \end{cases}.$$

This is written in vector form as

$$\mathbf{H}^- = \mathbf{H}^+, \tag{4}$$

$$S_1\mathbf{H}_x^- + S_2\mathbf{H}_y^- = S_3\mathbf{H}_x^+ + S_4\mathbf{H}_y^+, \tag{5}$$

where the matrices S are defined as

$$S_1 = \begin{pmatrix} 0 & -1/n_1^2 \\ 1 & 0 \end{pmatrix}, \quad S_2 = \begin{pmatrix} 1/n_1^2 & 0 \\ 0 & 1 \end{pmatrix},$$

$$S_3 = \begin{pmatrix} 0 & -1/n_2^2 \\ 1 & 0 \end{pmatrix}, \quad S_4 = \begin{pmatrix} 1/n_2^2 & 0 \\ 0 & 1 \end{pmatrix}.$$

The next step is to choose the point (x_i^*, y_j^*) which lies on the interface. Unlike the 1D case (see Appendix), here we have some flexibility in choosing these points and as such we choose to work with the closest point to (x_i, y_j).

After choosing (x_i^*, y_j^*) a local coordinate transformation is applied near this grid point. This will be a shift and a rotation. Let θ be the angle between the x-axis and the normal direction, pointing in the direction of the $(+)$ side. The transformation is defined as (cf. Fig. 1)

$$\xi = (x - x_i^*)\cos\theta + (y - y_j^*)\sin\theta, \tag{6a}$$

$$\eta = -(x - x_i^*)\sin\theta + (y - y_j^*)\cos\theta. \tag{6b}$$

Under transformation (6b) the system of differential equations remains unchanged, namely

$$\mathbf{H}_{\xi\xi} + \mathbf{H}_{\eta\eta} + k^2 n^2 H = \beta^2 \mathbf{H} \tag{7}$$

since

$$\frac{\partial^2}{\partial x^2} = \cos^2\theta \frac{\partial^2}{\partial \xi^2} + \sin^2\theta \frac{\partial^2}{\partial \eta^2} - 2\cos\theta\sin\theta \frac{\partial^2}{\partial \xi \partial \eta},$$

$$\frac{\partial^2}{\partial y^2} = \sin^2\theta \frac{\partial^2}{\partial \xi^2} + \cos^2\theta \frac{\partial^2}{\partial \eta^2} + 2\cos\theta\sin\theta \frac{\partial^2}{\partial \xi \partial \eta}.$$

This would not have been the case if we were to keep the term involving the derivatives of the refractive index. Instead, these terms are appropriately added to the fields' continuity conditions across each interface.

In the new coordinates the finite difference equation becomes

$$\Gamma_1 \mathbf{H}(\xi_1, \eta_1) + \Gamma_2 \mathbf{H}(\xi_2, \eta_2) + \Gamma_3 \mathbf{H}(\xi_3, \eta_3) + \Gamma_4 \mathbf{H}(\xi_4, \eta_4) + \Gamma_5 \mathbf{H}(\xi_5, \eta_5) + \Gamma_6 \mathbf{H}(\xi_6, \eta_6) = \beta^2 \mathbf{H}(\xi_3, \eta_3),$$

where the matrices Γ depend upon the matrices S and the rotation angle θ. Notice that an additional point must be added to the set to complete the square system. This new point is the one closest to (x_i^*, y_j^*) on the grid that does not already belong to the five stencil points of the scheme (labeled in Fig. 1 as "6"). Expanding all terms we have

$$\begin{aligned} &\Delta_1 \mathbf{H}^- + \Delta_2 \mathbf{H}^+ + \Delta_3 \mathbf{H}_\xi^- + \Delta_4 \mathbf{H}_\xi^+ + \Delta_5 \mathbf{H}_\eta^- + \Delta_6 \mathbf{H}_\eta^+ + \Delta_7 \mathbf{H}_{\xi\xi}^- + \Delta_8 \mathbf{H}_{\xi\xi}^+ + \Delta_9 \mathbf{H}_{\eta\eta}^- + \Delta_{10} \mathbf{H}_{\eta\eta}^+ + \Delta_{11} \mathbf{H}_{\xi\eta}^- + \Delta_{12} \mathbf{H}_{\xi\eta}^+ \\ &\quad = \mathbf{H}_{\xi\xi}^- + \mathbf{H}_{\eta\eta}^- + k^2 n_1^2 \mathbf{H}^- \end{aligned} \tag{8}$$

where we have used Eq. (7) to substitute for $\beta^2 \mathbf{H}^-$ and

$$\Delta_1 = \sum_{i\in(-)} \Gamma_i, \quad \Delta_5 = \sum_{i\in(-)} \eta_i \Gamma_i, \quad \Delta_9 = \frac{1}{2}\sum_{i\in(-)} \eta_i^2 \Gamma_i,$$

$$\Delta_2 = \sum_{i\in(+)} \Gamma_i, \quad \Delta_6 = \sum_{i\in(+)} \eta_i \Gamma_i, \quad \Delta_{10} = \frac{1}{2}\sum_{i\in(+)} \eta_i^2 \Gamma_i,$$

$$\Delta_3 = \sum_{i\in(-)} \xi_i \Gamma_i, \quad \Delta_7 = \frac{1}{2}\sum_{i\in(-)} \xi_i^2 \Gamma_i, \quad \Delta_{11} = \sum_{i\in(-)} \xi_i \eta_i \Gamma_i,$$

$$\Delta_4 = \sum_{i\in(+)} \xi_i \Gamma_i, \quad \Delta_8 = \frac{1}{2}\sum_{i\in(+)} \xi_i^2 \Gamma_i, \quad \Delta_{12} = \sum_{i\in(+)} \xi_i \eta_i \Gamma_i.$$

We need to substitute in (8) for the $(+)$ functions and find the systems the finite difference coefficients (the Γ matrices) must satisfy by comparing relative terms from each side of the equation (this becomes more clear below). For this we need six equations in total in the new coordinate system. Start with

$$\mathbf{H}^- = \mathbf{H}^+.$$

Differentiate twice with respect to η to get two additional equations at the interface

$$\mathbf{H}_\eta^- = \mathbf{H}_\eta^+,$$

$$\mathbf{H}_\xi^- \chi''(0) + \mathbf{H}_{\eta\eta}^- = \mathbf{H}_\xi^+ \chi''(0) + \mathbf{H}_{\eta\eta}^+.$$

The function χ is defined as $\xi = \chi(\eta)$ and its second derivative is the curvature at the specific point. Here we used

$$\frac{d}{d\eta} = \frac{d\xi}{d\eta}\frac{\partial}{\partial \xi} + \frac{\partial}{\partial \eta} = \chi'(0)\frac{\partial}{\partial \xi} + \frac{\partial}{\partial \eta},$$

since the point (x_i^*, y_j^*) is on the interface is the point (0,0) in the new coordinate system. Also it is apparent that $\chi(0) = \chi'(0) = 0$. An additional set of two equations will come from Eq. (5), which under the transformation (6) becomes

$$A_1 \mathbf{H}_\xi^- + A_2 \mathbf{H}_\eta^- = A_3 \mathbf{H}_\xi^+ + A_4 \mathbf{H}_\eta^+,$$

with

$$A_1 = \cos\theta S_1 + \sin\theta S_2 \quad A_3 = \cos\theta S_3 + \sin\theta S_4,$$
$$A_2 = -\sin\theta S_1 + \cos\theta S_2 \quad A_4 = -\sin\theta S_3 + \cos\theta S_4.$$

Again differentiating this with respect to η we get

$$A_1\mathbf{H}^-_{\xi\eta} + A_2\mathbf{H}^-_{\eta\eta} = A_3\mathbf{H}^+_{\xi\eta} + A_4\mathbf{H}^+_{\eta\eta}.$$

The final equation comes from the equation itself. Since the fields are continuous, namely $\beta^2\mathbf{H}^- = \beta^2\mathbf{H}^+$, it follows that

$$\mathbf{H}^-_{\xi\xi} + \mathbf{H}^-_{\eta\eta} + k^2n_1^2\mathbf{H}^- = \mathbf{H}^+_{\xi\xi} + \mathbf{H}^+_{\eta\eta} + k^2n_2^2\mathbf{H}^+.$$

And thus we have enough equations to substitute for. Substituting for the $(+)$ functions from the continuity conditions into Eq. (8), namely

$$\mathbf{H}^+ = \mathbf{H}^-,$$
$$\mathbf{H}^+_\eta = \mathbf{H}^-_\eta,$$
$$\mathbf{H}^+_\xi = A_3^{-1}A_1\mathbf{H}^-_\xi + A_3^{-1}(A_2 - A_4)\mathbf{H}^-_\eta,$$
$$\mathbf{H}^+_{\eta\eta} = \mathbf{H}^-_{\eta\eta} + \chi''(0)(I_2 - A_3^{-1}A_1)\mathbf{H}^-_\xi - \chi''(0)A_3^{-1}(A_2 - A_4)\mathbf{H}^-_\eta,$$
$$\mathbf{H}^+_{\xi\eta} = A_3^{-1}A_1\mathbf{H}^-_{\xi\eta} - A_3^{-1}(A_4 - A_2)\mathbf{H}^-_{\eta\eta} - \chi''(0)A_3^{-1}A_4(I_2 - A_3^{-1}A_1)\mathbf{H}^-_\xi + \chi''(0)A_3^{-1}A_4A_3^{-1}(A_2 - A_4)\mathbf{H}^-_\eta,$$
$$\mathbf{H}^+_{\xi\xi} = \mathbf{H}^+_{\xi\xi} - \chi''(0)(I_2 - A_3^{-1}A_1)\mathbf{H}^-_\xi + \chi''(0)A_3^{-1}(A_2 - A_4)\mathbf{H}^-_\eta - k^2(n_2^2 - n_1^2)\mathbf{H}^-$$

and equating coefficients of the relative terms of $\mathbf{H}^-$ and its derivatives from the left and right hand sides of Eq. (8) we obtain the following system

$$\Delta_1 + \Delta_2 - k^2(n_2^2 - n_1^2)\Delta_8 = k^2n_1^2I_2,$$
$$A_3^{-1}(A_2 - A_4)\Delta_4 + \Delta_5 + \Delta_6 + \chi''(0)A_3^{-1}(A_2 - A_4)\Delta_8 - \chi''(0)A_3^{-1}(A_2 - A_4)\Delta_{10} + \chi''(0)A_3^{-1}A_4A_3^{-1}(A_2 - A_4)\Delta_{12} = \mathbb{O},$$
$$\Delta_3 + A_3^{-1}A_1\Delta_4 - \chi''(0)(I_2 - A_3^{-1}A_1)\Delta_8 + \chi''(0)(I_2 - A_3^{-1}A_1)\Delta_{10} - \chi''(0)A_3^{-1}A_4(I_2 - A_3^{-1}A_1)\Delta_{12} = \mathbb{O},$$
$$\Delta_9 + \Delta_{10} + A_3^{-1}(A_2 - A_4)\Delta_{12} = I_2,$$
$$\Delta_7 + \Delta_8 = I_2,$$
$$\Delta_{11} + A_3^{-1}A_1\Delta_{12} = \mathbb{O},$$

where $\mathbb{O}$ is the 2×2 zero matrix.

In a similar manner the system after substituting for the $(-)$ functions is

$$\Delta_1 + \Delta_2 + k^2(n_2^2 - n_1^2)\Delta_7 = k^2n_2^2I_2,$$
$$A_1^{-1}(A_4 - A_2)\Delta_3 + \Delta_5 + \Delta_6 + \chi''(0)A_1^{-1}(A_4 - A_2)\Delta_7 - \chi''(0)A_1^{-1}(A_4 - A_2)\Delta_9 + \chi''(0)A_1^{-1}A_2A_1^{-1}(A_4 - A_2)\Delta_{11} = \mathbb{O},$$
$$A_1^{-1}A_3\Delta_3 + \Delta_4 - \chi''(0)(I_2 - A_1^{-1}A_3)\Delta_7 + \chi''(0)(I_2 - A_1^{-1}A_3)\Delta_9 - \chi''(0)A_1^{-1}A_2(I_2 - A_1^{-1}A_3)\Delta_{11} = \mathbb{O},$$
$$\Delta_9 + \Delta_{10} + A_1^{-1}(A_4 - A_2)\Delta_{11} = I_2$$
$$\Delta_7 + \Delta_8 = I_2,$$
$$A_1^{-1}A_3\Delta_{11} + \Delta_{12} = \mathbb{O}.$$

These systems of algebraic equations determine the coefficients of the matrices at all irregular points. If multiple interfaces are present, one merely applies these formulas multiple times. Note that the result is a system of finite difference equations each involving six neighboring points which does not add additional elements to the FD matrix; one only corrects elements according to these systems. Because of this structure of the matrix, sparse matrix algebra can be used to determine the eigenvalues and eigenmodes. Thus, a large number of points can be used with modest computational cost, which allows the accuracy of the results to be increased and the modes of complicated structures to be determined. Also note that the corrections depend only on the values of the refractive index before and after the discontinuity. This means that the jump conditions do not have to be modified if the index varies between the discontinuities.

4. Waveguide analysis

4.1. Step-index fibers

The first example we consider is the fundamental modes of a step-index fiber. This fiber has a solid core with index $n_1 = 3$ of radius $r = 1$, a cladding with index $n_2 = 1.5$, and wavelength 2π (i.e. $k = 1$). The exact propagation constant is 2.269700. We ran our code for different numbers of points and the results are summarized in Table 1.

A few comments are in order. The results above seem a less accurate than the 1D case, but recall that in the 2D case we need to diagonalize an $n \times n$ where n is the number of points per dimension. The use of sparse matrix algebra is essential.

Table 1
Propagation constants for the fundamental mode of a circular step-index fiber.

Number of points per dimension	20	30	40	60
Propagation constant	2.255329	2.258572	2.266226	2.267538
Relative error	0.0063	0.0049	0.0015	0.00095

When employing the immersed interface method, one needs to be careful not to loose this property of the matrix. Another point worth noting concerns the extra point we need, the point labeled "6" in the finite difference scheme (see Fig. 1). This point is not always in the same place as in the figure above. Any of the points diagonally across from "3" could be the new point depending on the position of "3". We also intentionally keep the number of points low to demonstrate the accuracy. Namely even for 20 points per dimension the relative error is kept to the order of $10^{-3} - 10^{-2}$.

The main advantage of this 2D IIM is that arbitrarily-shaped interfaces can be used. As an example, consider an elliptical waveguide with semi-major axis $\sqrt{2}$ and semi-minor axis $1/\sqrt{2}$ (so that the cross-sectional area of the waveguide is the same as the circular waveguide given above). With a core index of 3 and a cladding index of 1.5, the IIM code gives the propagation constants as in Table 2.

The doubly-degenerate eigenmode of the circular waveguide has now been split into two different modes with different propagation constants.

To further demonstrate, we consider a step-index fiber whose shape is described by a limaçon $r = b + a\cos\theta$ with parameters $a = \sqrt{2}/3$ and $b = 2a$ such that its total area is π, the same as the area of the unit circle, as above. This particular problem cannot be solved analytically and no direct comparison can be made. The index of refraction is $n_1 = 3$ inside the fiber and $n_2 = 1.5$, outside. The modes for the circular case with the same characteristics are degenerate and the highest eigenvalue is 2.26864 [9]. In this case, the degeneracy is lifted and the modes separate with eigenvalues 2.28649 and 2.24815, respectively. The first modes of this fiber are shown in Fig. 2. Note that the limaçon is not centered at the origin.

Table 2
Propagation constants for an elliptical step-index fiber.

Number of points per dimension	60
Propagation constants	2.328580
	2.030432

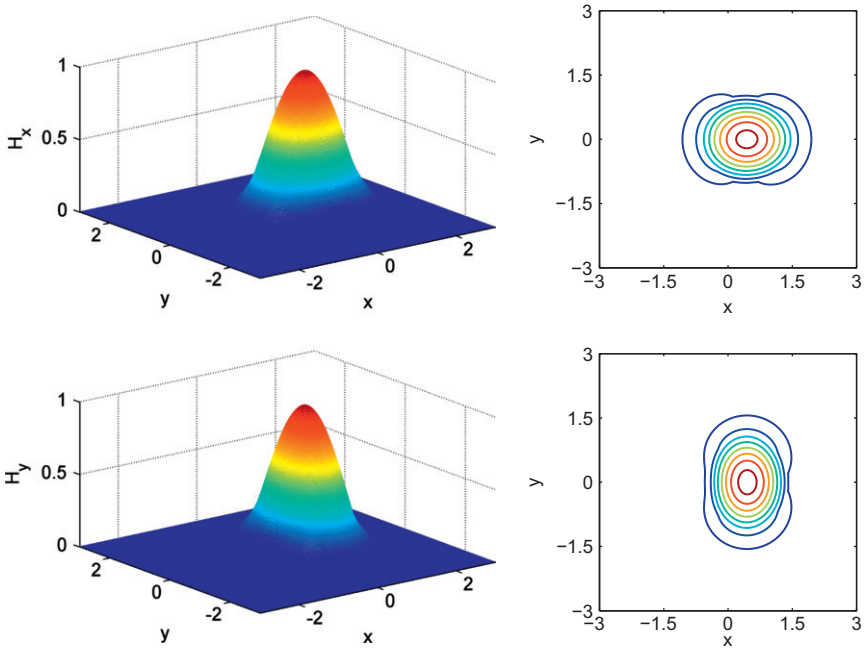

Fig. 2. The first two modes corresponding to the limaçon step-index fiber.

4.2. Multilayered fibers

The main difficulty here is that the step of the finite difference approximation must be chosen such that we have at least two points between the layers so that a specific point will not be an irregular point for both interfaces (cf. Fig. 3).

On the left figure the point labeled "6" is an irregular point for both interfaces (the IIM will fail in this case). The right figure shows geometry in which the IIM can be applied. A sufficiently large number of grid points must be used so that this problem is avoided. Because the reflecting layers are small many more points will be used in the core region than necessary, i.e., the core region will be over-resolved. This adds significant computational cost; in the case of a 2-D problem, this added computational cost can be quite large.

As an example of a multilayered fiber consider a Bragg fiber that has an air core of radius 5 μm and 15 alternate layers of radius 1 μm and refractive indices 2 and 1, respectively. The effective index of the TE mode is found to be 0.785771. The field is shown in Fig. 4.

A slice along the x and y axes gives the H_x and H_y components in Fig. 5.

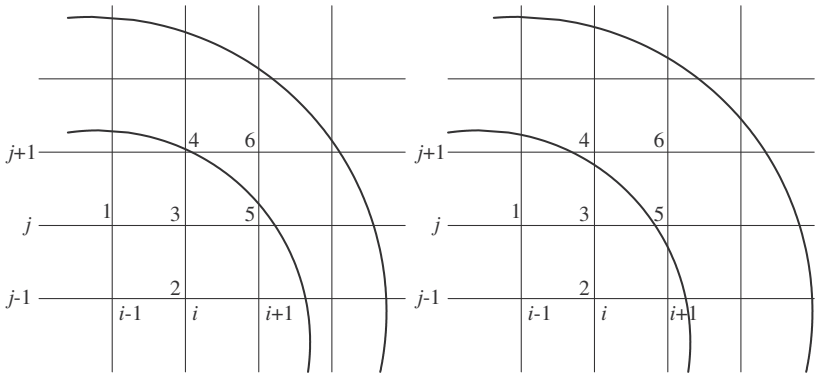

Fig. 3. The two possible grid cases. On the left the IIM fails, while it can be applied on the right.

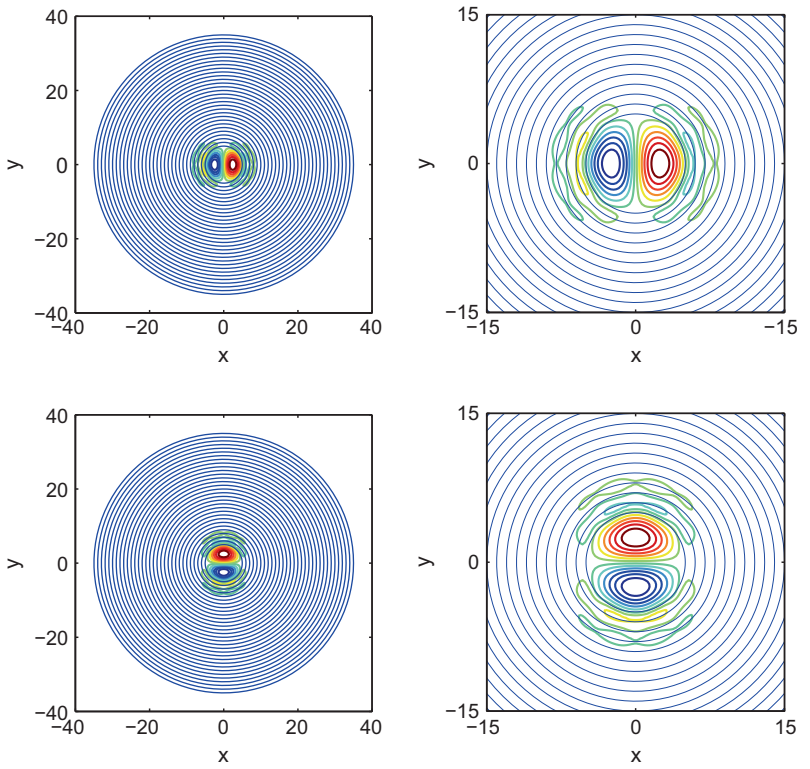

Fig. 4. The first eigenmode of a circular Bragg fiber. The top contours gives the x component of the field (full scale, left, and zoomed, right), while the bottom contours give the y component.

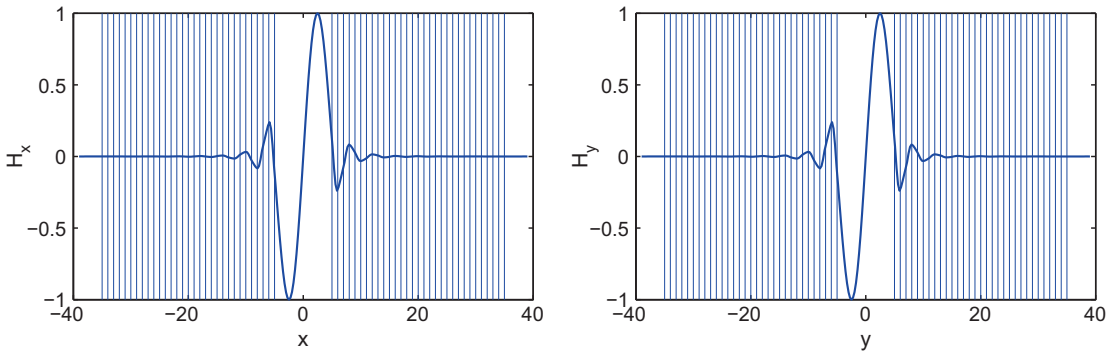

Fig. 5. 1D slices of the Bragg fiber showing the TE mode.

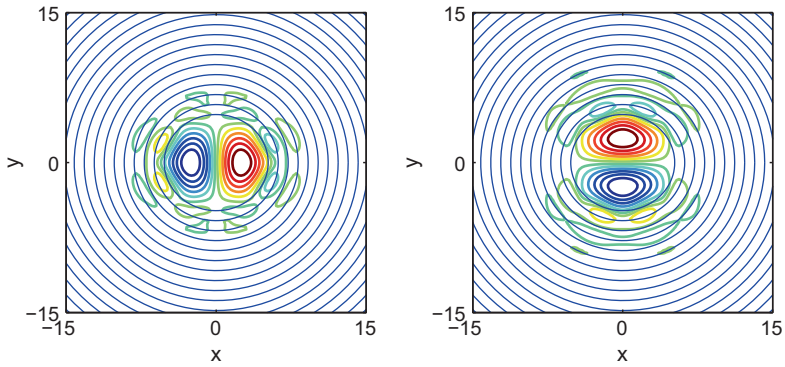

Fig. 6. The first eigenmode of an elliptical Bragg fiber.

To further demonstrate the ability of the method to handle arbitrary 2D shapes, we model a slightly elliptical fiber similar to the above circular fiber; we merely stretch one axis slightly from the circular case so that the major axis of the ellipse is now $r_i + 0.2$, where r_i are the radii of above circles. The first eigenmode is shown in Fig. 6, with corresponding eigenvalue 0.782961.

5. Conclusions

To conclude, we have described a numerical technique based on finite differences to analyze the guided vector modes of a waveguide with arbitrary cross section and arbitrary index of refraction. Cumbersome integrations or finding roots of non-trivial functions, such as Bessel and Mathieu functions, are avoided and computational time is kept to a minimum without sacrificing accuracy. All modes can be determined and excellent results are achieved even for fibers with complicated structures. Notably, this method finds application to other problems of physical importance like the study of semiconductors and quantum well structures [28,29].

One of the key results is the reformulation of the immersed interface method in vector form. This vector form significantly reduces the complexity associated with implementing the algorithm, and was essential for the extension of the method to the 2D coupled equations.

Acknowledgement

I am very grateful to W.L. Kath for his help and support concerning this work.

Appendix A. The 1D radially symmetric case

Assume that the mode fields have the form [23,24]

$$\mathbf{E}(r,\theta,z,t) = \mathbf{e}(r,\theta)e^{i(\beta z-\omega t)} \quad \mathbf{B}(r,\theta,z,t) = \mathbf{b}(r,\theta)e^{i(\beta z-\omega t)},$$

where β is the propagation constant of the mode. Maxwell's equations can be written for for the two components of the magnetic field (b_r, b_θ) as

$$\frac{1}{r}\frac{\partial}{\partial r}\left(r\frac{\partial b_r}{\partial r}\right)+\frac{1}{r^2}\left(\frac{\partial^2 b_r}{\partial\theta^2}-b_r-2\frac{\partial b_\theta}{\partial\theta}\right)+\left(\frac{\omega n}{c}\right)^2 b_r=\beta^2 b_r,$$

$$\frac{n^2}{r}\frac{\partial}{\partial r}\left[\frac{1}{n^2}\left[\frac{\partial}{\partial r}(rb_\theta)-\frac{\partial b_r}{\partial\theta}\right]\right]+\frac{1}{r^2}\left[\frac{\partial^2 b_\theta}{\partial\theta^2}-b_\theta+2\frac{\partial b_r}{\partial\theta}\right]-\frac{1}{r}\frac{\partial}{\partial r}\left(b_\theta-\frac{\partial b_r}{\partial\theta}\right)+\left(\frac{\omega n}{c}\right)^2 b_\theta=\beta^2 b_\theta.$$

Suppose that $b_r(r,\theta)=b_{rm}(r)\cos(m\theta)$ and $b_\theta(r,\theta)=b_{\theta m}(r)\sin(m\theta)$ with $m\geqslant 1$. Then

$$b_r''+\frac{1}{r}b_r'+\left(k^2n^2-\frac{m^2+1}{r^2}\right)b_r=\beta^2 b_r+\frac{2m}{r^2}b_\theta, \quad \text{(A.1a)}$$

$$b_\theta''+\left(-\frac{2n'}{n}+\frac{1}{r}\right)b_\theta'+\left(k^2n^2-\frac{m^2+1}{r^2}-\frac{2n'}{nr}\right)b_\theta=\beta^2 b_\theta+m\left(\frac{2n'}{nr}+\frac{2}{r^2}\right)b_r, \quad \text{(A.1b)}$$

where the primes denote differentiation with respect to r. Here, we have substituted for the angular dependence, dropped the subscript m and rearranged terms.

The refractive index has a jump at, say, $r=r^*$, so that

$$n(r)=\begin{cases} n_1, & r<r^*,\\ n_2, & r>r^*.\end{cases}$$

What one normally would consider is a finite difference approximation for Eq. (A.1b) of the form

$$\gamma_1 b_{r,i-1}+\gamma_2 b_{r,i}+\gamma_3 b_{r,i+1}+\Delta b_{\theta,i}=\beta^2 b_{r,i},$$
$$\delta_1 b_{\theta,i-1}+\delta_2 b_{\theta,i}+\delta_3 b_{\theta,i+1}+\Gamma b_{r,i}=\beta^2 b_{\theta,i},$$

where

$$\gamma_1=\delta_1=\frac{1}{h^2}-\frac{1}{2hr_i},\quad \gamma_2=\delta_2=-\frac{2}{h^2}+k^2n^2-\frac{1}{r_i^2},\quad \gamma_3=\delta_3=\frac{1}{h^2}+\frac{1}{2hr_i},\quad \Gamma=\Delta=-\frac{2m}{r_i^2},$$

with $r\in[a,b]$ defined on a uniform grid as

$$r_i=a+ih=a+i\left(\frac{b-a}{N}\right),\quad i=0,1,2,\ldots,N.$$

Instead we reformulate the problem, including the differential equations, in vector form. In addition, the terms including derivatives of discontinuous functions are neglected (we assume the index is piecewise constant) and their contribution is incorporated into the finite difference scheme. Thus, Eq. (A.1) are

$$\mathbf{u}_{rr}+\frac{1}{r}\mathbf{u}_r+B\mathbf{u}=\beta^2\mathbf{u},$$

where $\mathbf{u}=(b_r,b_\theta)^{\mathbf{T}}$, and

$$B=\begin{pmatrix} k^2n^2-\frac{m^2+1}{r^2} & -\frac{2m}{r^2}\\ -\frac{2m}{r^2} & k^2n^2-\frac{m^2+1}{r^2}\end{pmatrix}$$

and the subscripts on vectors denote differentiation. The continuity conditions in vector form are [23,24]

$$\mathbf{u}^+=\mathbf{u}^-,$$
$$\mathbf{u}_r^+=C\mathbf{u}_r^-+D\mathbf{u},$$
$$\mathbf{u}_{rr}^+=\mathbf{u}_{rr}^-+E\mathbf{u}_r^-+F\mathbf{u},$$

with

$$C=\begin{pmatrix}1 & 0\\ 0 & \frac{n_2^2}{n_1^2}\end{pmatrix},\quad D=\frac{n_2^2/n_1^2-1}{r^*}\begin{pmatrix}0 & 0\\ m & 1\end{pmatrix},$$

$$E=-\frac{n_2^2/n_1^2-1}{r^*}\begin{pmatrix}0 & 0\\ 0 & 1\end{pmatrix},\quad F=-\begin{pmatrix}k(n_2^2-n_1^2) & 0\\ m\frac{n_2^2/n_1^2-1}{r^*2} & \frac{n_2^2/n_1^2-1}{r^{*2}}+k(n_2^2-n_1^2).\end{pmatrix}$$

The finite difference approximation in matrix form is

$$\Gamma_1\mathbf{u}_{i-1}+\Gamma_2\mathbf{u}_i+\Gamma_3\mathbf{u}_{i+1}=\beta^2\mathbf{u}_i,$$

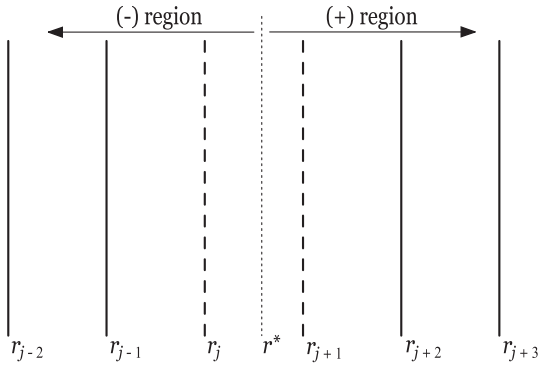

Fig. A.7. The $(-)$ and $(+)$ regions, the problematic point $r = r^*$ and the irregular grid points r_j and r_{j+1}.

where the scalar coefficients, γ_i, are replaced by the 2×2 matrices Γ. We need to expand $\mathbf{u}_{i-1}, \mathbf{u}_i$ and $\mathbf{u}_{i+1}$ around the points of the grid that include r^*. Say that $r_j < r^* < r_{j+1}$, the $(-)$ and $(+)$ regions are on the left and right of r^*, respectively, as portrayed in Fig. A.7.

Replacing the $(-)$ and $(+)$ values of the fields using the matching conditions and equating relevant coefficients, the systems that determine the finite difference corrections at these regions are at $r_j < r^*$

$$\Gamma_1 + \Gamma_2 + \Gamma_3\left[I_2 + (r_{j+1} - r^*)D + \frac{1}{2}(r_{j+1} - r^*)^2 F\right] = B^-,$$
$$(r_{j-1} - r^*)\Gamma_1 + (r_j - r^*)\Gamma_2 + \Gamma_3\left[(r_{j+1} - r^*)C + \frac{1}{2}(r_{j+1} - r^*)^2 E\right] = \frac{1}{r^*} I_2,$$
$$\frac{1}{2}(r_{j-1} - r^*)^2\Gamma_1 + \frac{1}{2}(r_j - r^*)^2\Gamma_2 + \frac{1}{2}(r_{j+1} - r^*)^2\Gamma_3 = I_2$$

and at $r_{j+1} > r^*$

$$\Gamma_1\left[I_2 - (r_j - r^*)C^{-1}D + \frac{1}{2}(r_j - r^*)^2 F_2\right] + \Gamma_2 + \Gamma_3 = B^+,$$
$$\Gamma_1\left[(r_j - r^*)C^{-1} + \frac{1}{2}(r_j - r^*)^2 E_2\right] + (r_{j+1} - r^*)\Gamma_2 + \Gamma_3(r_{j+2} - r^*) = \frac{1}{r^*} I_2,$$
$$\frac{1}{2}(r_j - r^*)^2\Gamma_1 + \frac{1}{2}(r_{j+1} - r^*)^2\Gamma_2 + \frac{1}{2}(r_{j+2} - r^*)^2\Gamma_3 = I_2,$$

where we need to introduce the matrices

$$E_2 = \begin{pmatrix} 0 & 0 \\ 0 & \frac{1-n_1^2/n_2^2}{r^*} \end{pmatrix}, \quad F_2 = \begin{pmatrix} k^2(n_2^2 - n_1^2) & 0 \\ m\frac{1-n_1^2/n_2^2}{r^*} & k^2(n_2^2 - n_1^2) - \frac{1-n_1^2/n_2^2}{r^{*2}} \end{pmatrix}$$

and I_2 is the 2×2 unit matrix.

For more details on the 1D case we refer the reader to Refs. [23,24].

References

[1] P. Yeh, A. Yariv, E. Marom, Theory of Bragg fiber, J. Opt. Soc. Am. 68 (1978) 1196–1201.
[2] Y. Fink, J.N. Winn, F. Shanhui, J.M.C. Chiping, J.D. Joannopoulos, E.L. Thomas, A dielectric omnidirectional reflector, Science 282 (1998) 1679–1682.
[3] B. Temelkuran, S.D. Hart, G. Benolt, J.D. Joannopoulos, Y. Fink, Wavelength-scalable hollow optical fibres with large photonic bandgaps for CO_2 laser transmission, Nature 420 (2002) 650–653.
[4] M. Ibanescu, Y. Fink, S. Fan, E.L. Thomas, J.D. Joannopoulos, An all-dielectric coaxial waveguide, Science 289 (2000) 415–419.
[5] S.G. Johnson, M. Ibanescu, M. Skorobogatiy, O. Weisberg, T.D. Engeness, M. Soljacic, S.A. Jacobs, J.D. Joannopolos, Y. Fink, Analysis of mode structure in hollow dielectric waveguide fibers, Opt. Express 9 (2001) 748–779.
[6] Y. Xu, R.K. Lee, A. Yariv, Asymptotic analysis of Bragg fibers, Opt. Lett. 25 (2000) 1756–1758.
[7] S. Guo, S. Albin, Comparative analysis of Bragg fibers, Opt. Express 12 (2004) 198–207.
[8] T. Kawanishi, M. Izutsu, Coaxial periodic optical waveguide, Opt. Express 7 (2000) 10–22.
[9] S. Guo, F. Wu, K. Ikram, S. Albin, Analysis of circular fibers with an arbitrary index profile by the Galerkin method, Opt. Lett. 29 (2004) 32–34.
[10] J.K. Shaw, A.M. Vengsarkar, R.O. Claus, Direct numerical analysis of dual-mode elliptical-core optical fibers, Opt. Lett. 16 (1991) 135–137.
[11] A. Kumar, R.K. Varshney, Propagation characteristics of dual-mode elliptical-core optical fibers, Opt. Lett. 14 (1989) 817–819.
[12] K. Thyagarajan, S.N. Sarkar, B.P. Pal, Equivalent step index (ESI) model for elliptic core fibers, J. Lightwave Technol. LT-5 (1987) 1041–1044.
[13] D. Kumar, I.O.N. Singh, Modal characteristic equation and dispersion curves for an elliptical step-index fiber with a conducting helical winding on the core-cladding boundary – an analytical study, J. Lightwave Technol. 20 (2002) 1416–1424.
[14] A.B. Fallahkhair, K.S. Li, T.E. Murphy, Vector finite difference modesolver for anisotropic dielectric waveguides, J. Lightwave Technol. 26 (2008) 1423–1431.

[15] C. Yeh, Elliptical dielectric waveguides, J. Appl. Phys. 33 (1962) 3235–3243.
[16] R.B. Dyott, Elliptical Fiber Waveguides, Artech House Publishers, 1995.
[17] L. Eyges, P. Gianino, P. Wintersteiner, Modes of dielectric waveguides of arbitrary cross sectional shape, J. Opt. Soc. Am. 69 (1979) 1226–1235.
[18] D. Marcuse, Solution of the vector wave equation for general dielectric waveguides by the Galerkin method, IEEE J. Quant. Elec. 28 (1992) 459–465.
[19] A.W. Snyder, X.H. Zheng, Optical fibers of arbitrary cross sections, J. Opt. Soc. Am. A 3 (1986) 600–609.
[20] C. Yeh, K. Ha, S.B. Dong, W.P. Brown, Single-mode optical waveguides, Appl. Opt. 18 (1979) 1490–1504.
[21] Z. Li, An overview of the immersed interface method and its applications, Taiwanese J. Math. 7 (2003) 1–49.
[22] R.J. Leveque, Z. Li, The immersed interface method for elliptic equations with discontinuous coefficients and singular sources, SIAM J. Numer. Anal. 31 (1994) 1019–1044.
[23] T.P. Horikis, W.L. Kath, Modal analysis of circular Bragg fibers with arbitrary index profiles, Opt. Lett. 31 (2006) 3417–3419.
[24] T.P. Horikis, Analysis of optical waveguides with arbitrary index profile using an immersed interface method, Int. J. Mod. Phys. C. 22 (2011) 687–710.
[25] S. Zhao, High order matched interface and boundary methods for the Helmholtz equation in media with arbitrarily curved interfaces, J. Comput. Phys. 229 (2010) 3155–3170.
[26] Y.-P. Chiou, C.-H. Du, Arbitrary-order full-vectorial interface conditions and higher order finite-difference analysis of optical waveguides, J. Lightwave Technol. 29 (2011) 3445–3452.
[27] W. Snyder, J.D. Love, Optical Waveguide Theory, Chapman & Hall, 1983.
[28] T.P. Horikis, Eigen state calculation of arbitrary quantum structures, Phys. Lett. A 359 (2006) 345–348.
[29] D.J. Costinett, T.P. Horikis, High-order eigenstate calculation of arbitrary quantum structures, J. Phys. A Math. Theor. 42 (2009) 235201.